Experimental and analytical validation of plain and reinforced concrete mine seal designs

K.M. Mohamed*, R.K. Zipf, D.F. Gearhart and T.J. Batchler
Researcher, senior mining engineer, electrical engineer and mechanical engineer, respectively, National Institute for Occupational Safety and Health, Pittsburgh, PA
*Email: kmy1@cdc.gov

Abstract

Seals are explosion-resistant structures built in underground coal mines to isolate abandoned mining areas from the active workings. An equivalent single degree of freedom (SDOF) method such as the single-degree-of-freedom blast effects design spreadsheet (SBEDS) developed by the U.S. Army Corps of Engineers can be used to design seals to resist mine explosions. The critical input for the SDOF code is the seal resistance function. The objective for this study is to develop engineering data for design of plain concrete (PC) and reinforced concrete (RC) seals using finite element (FE) models. The FE models can then be used to generate resistance functions for different PC and RC seal designs, which can be used in the SDOF codes. The U.S. National Institute for Occupational Safety and Health (NIOSH) researchers designed and built a test fixture for use in conjunction with NIOSH's Mine Roof Simulator to apply a four-point bending load on the face of the tested seal. Eight large-scale experiments for each PC and RC seal were conducted. The experimental design considered the effects of the foundation strength, hitching and roof-to-floor convergence. Calibrated FE models for PC and RC seals were developed using ANSYS Ver. 13. With a very limited number of engineering-based assumptions and a single set of data—including Young's modulus, compressive strength, stress-strain relationships, etc.—the PC and RC seal models successfully calculated the recorded resistance functions and failure patterns for a wide range of boundary conditions. Plug and RC seals were assumed for a 1.83-m- (6-ft-) high entry to demonstrate the application of the calibrated finite element models for calculating the resistance functions of these seals. The resistance function of a particular plug seal case was found to be a bilinear relationship. The resistance function of a particular RC seal without shear reinforcement was found to be a nonlinear relationship.

Key words: Coal, Modeling and simulation, Mine seals

2013 *Transactions of the Society for Mining, Metallurgy and Exploration*, Vol. 334, pp. 477-488.

Introduction

Seals are used in underground coal mines throughout the United States to isolate abandoned mining areas from the active workings. Prior to the Sago Mine disaster in 2006, mining regulations required seals to withstand a 0.14-MPa (20-psi) explosion pressure. Current mining regulations (30 CFR 75.335(a)) require that seal designs resist a pressure-time curve with an instantaneous peak explosion pressure of 0.35 or 0.83 MPa (50 or 120 psi), depending on the seal application (*Federal Register*, 2008). A number of these approved seal designs are posted on the U.S. Mine Safety and Health Administration (MSHA) website (MSHA, 2012). The approved seals can be classified into four groups: plain concrete seals, reinforced concrete seals, pumpable cement foam seals and seals made from concrete masonry units glued with polymer.

Static and dynamic analysis methods can be used to design seals to resist mine explosions. Three distinct methods for mine seal design are summarized:

1. *Equivalent static method* - The simplest method for designing a structure subject to a dynamic load is the equivalent static analysis method, in which the applied dynamic load is transformed into an equivalent static load using a dynamic load factor (DLF). The DLF is the ratio of the dynamic deflection at any time to the static deflection resulting from the load used in specifying the load-time curve. The DLF depends on the shape of the applied dynamic load-time curve and accounts for inertial effects in the design. The allowable loads and stresses are also modified to consider the dynamic effects using a dynamic increase factor (DIF). In linear elastic systems, deflections, forces and stresses are all linearly proportional; therefore, the DLF applies to any of these quantities to determine the ratio of dynamic to static effects. In many structural problems, only the maximum value of the DLF is of interest. The maximum displacements, forces and stresses due to the dynamic load are twice the value that would be obtained from a static analysis for the maximum load. The pressure-time curves with instantaneous rise time listed in 30 CFR 75.335(a) require a DLF of 2.0 (*Federal Register*, 2008).
2. *Equivalent single degree of freedom system (SDOF)*

Paper number TP-13-003. Original manuscript submitted January 2013. Revised manuscript accepted for publication July 2013. Discussion of this peer-reviewed and approved paper is invited and must be submitted to SME Publications Dept. prior to Sept. 30, 2014.

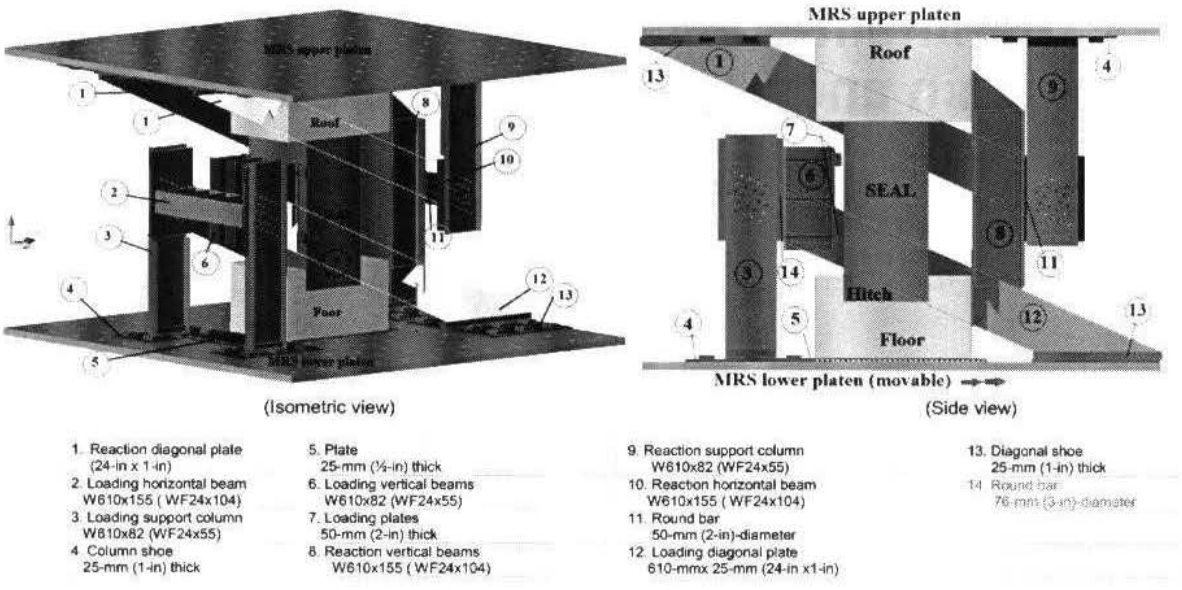

Figure 1 — MRS seal testing fixture and seal model inside the MRS.

method - Mine seals can be represented with an equivalent SDOF system. The dynamic equilibrium equation of the SDOF system can be solved either graphically using nondimensional charts and graphs (Army, 1990) or using a numerical integration technique as in the single-degree-of-freedom blast effects design spreadsheet (SBEDS) (Army Corps of Engineers, 2013).

3. Numerical modeling techniques - Finite element, finite difference, distinct element and discrete element techniques have been used to analyze the dynamic response of mine seals subjected to explosion pressures (Mohamed et al., 2009; Kallu et al., 2007; Gadde et al., 2008; Mutton and Remennikov, 2010; Westman, 2007).

The numerical modeling technique is the most realistic approach for analyzing explosion-resistant structures, because it accounts for the multiple degree of freedom and complex boundary conditions of the structures. But the effort associated with the development of numerical models and interpretation of results is often greater than what is required by the SDOF method (American Society of Civil Engineers, 2007). Therefore, including the numerical technique in the SDOF code would be the most suitable method for mine seal analysis and design, if an appropriate seal resistance function is available. The seal resistance function describes the lateral load-bearing capacity versus the center-point displacement for the seal. Resistance functions of mine seals can be determined from experiments on seal structures (Zipf et al., 2009) or calculated using numerical modeling techniques. The resistance function of mine seals depends on the seal geometry, construction material, foundation strength (roof, floor and ribs) and support condition (hitching).

The objectives of this seal testing program are to derive the resistance functions of PC and RC seals by conducting large-scale static tests and, then, comparing these resistance functions with those calculated with finite element analysis. Four major factors were considered in the seal testing program: (1) construction material, (2) foundation conditions, (3) hitching conditions and (4) roof-to-floor convergence. The results of the test program provided the validation data to calibrate finite element models which were used to generate the resistance functions for SDOF codes such as SBEDS (Army Corps of Engineers, 2013).

New mine seal testing method

NIOSH researchers proposed a new testing method for evaluating the strength of large-scale mine seals (Zipf and Mohamed, 2009). The method is based on the four-point flexural test suggested by the ASTM E72-02 for conducting strength tests of panels for building construction (ASTM, 2002). The four-point test is a good approximation of a uniformly loaded seal. Based on this ASTM method, NIOSH researchers designed a seal testing fixture using a four-point load, which is applied until failure to 1.22-m- (4-ft-) wide by 1.83-m- (6-ft-) high seals.

For seals designed using the 0.83-MPa (120-psi) pressure-time curve with instantaneous rise time, the equivalent static pressure is 1.66 MPa (240 psi). Assuming a 1.22-m- (4-ft-) wide by 1.83-m- (6-ft-) high seal loaded with a uniform pressure of 1.66 MPa (240 psi), the equivalent force is 37 MN (830,000 lbf). A lateral design load of 40 MN (900,000 lbf) was selected for the design of the testing fixture.

Figure 1 shows a drawing of the seal and testing fixture mounted in the mine roof simulator (MRS). The seal model consists of the 1.22-m- (4-ft-) wide by 1.83-m- (6-ft-) high seal, as well as the roof and floor foundation blocks. The foundation blocks measure 1.22-m (4-ft) wide by 1.01-m (3.33-ft) high by 1.52-to-2.54-m (5-to-8.33-ft) long. The thickness of the seal varies depending on the construction material. The total height of the seal model including the foundation blocks is 3.86 m (12.7 ft). Hereafter, the term "seal model" refers to the test seal along with the roof and floor foundations. The foundations and seals are cast from commercial concrete with properties listed in Table 1. The floor foundation may or may not contain a notch to simulate floor hitching.

The MRS seal testing fixture shown in Fig. 1 is composed of two similar opposing frames, one for load application and the other to provide the reaction. The frames are fabricated from steel of tensile strength 248 MPa (36,000 psi). The reaction (top) frame of the MRS seal testing fixture is stationary,

Table 1 — Material properties for PC and RC finite element seal models. Green cells are laboratory-measured properties, blue cells are empirically calculated properties, gray cells are properties calculated from the MRS seal tests and orange cells are assumed properties.

Material properties		Seal		Strong floor (S)		Roof		Weak floor (W)	
		PC	RC	PC/Plug	RC	PC	RC/Plug	PC	RC
Concrete specification	w/c ratio	0.47		0.45		0.5	0.35	0.42	1.64
	c:s:a ratio	1:2.7:3		1:1.2:3.1		1:2.4:4.4	1:2.5:3.6	1:3:4.3	1:11:12
Young's modulus, GPa (x10^6 psi)		9.10 (1.32)		9.93 (1.44)		9.93 (1.44)	7.79 (1.13)	4.83 (0.7)	1.24 (0.18)
Tensile strength, f_r, MPa (psi)		1.03** (150)	3.25* (472)	3.79* (550)		3.78* (548)	3.34* (430)	2.37* (344)	1.37* (199)
Compressive strength, f_c, MPa (psi)		29.1 (4,220)		36.7 (5,330)		35.6 (5,170)	22.7 (3,290)	14.6 (2,100)	4.36 (632)
Seal/roof and seal/floor interface	Shear stiffness, MPa/mm (psi/in.)	-		1.28 (4,730)		0.96 (3,550)		0.87 (3,200)	
	Cohesion, MPa (psi)	-		1.95 (283)		3.22 (467)		1.95 (283)	0.34 (50)
	Friction coefficient	-		0.8	0.45	0.8	0.45	0.8	0.4

**Equation (1)

* Equation (2)

w/c ratio = water to cement ratio by weight

c:s:a ratio = cement : sand : coarse aggregate ratio by weight

while the loading (bottom) frame moves horizontally along with the lower platen of the MRS. The main concept of the MRS seal testing fixture is to use the vertical loading capability of the MRS to simulate a roof-to-floor convergence load on a seal and the horizontal loading capability of the MRS to apply static load on the face of the seal. With reference to Fig. 1, the loading and reaction frames include horizontal beams (parts 2 and 10) connected to support columns (parts 3 and 9) and diagonal plates (parts 1 and 12). The support columns and diagonals are welded into 25-mm- (1-in.-) thick steel plates (shoes – parts 4 and 13), which are fastened in the platens of the MRS by seventy 76-mm- (3-in.-) diameter bolts. The vertical loading and reaction beams (parts 6 and 8) are hung from the horizontal loading and reaction beams (parts 2 and 10). The vertical loading and reaction beams rotate freely around horizontal bars (parts 11 and 14). The applied load on the face of the seal is developed by the horizontal actuators located under the lower platen of the MRS. This force is transferred to the horizontal and vertical loading beams via the diagonal loading plates on both sides of the seal model. The horizontal force is applied on the loading face of the seal via two loading plates (part 7). Rollers under a plate (part 5) are placed underneath the floor block of the model to ensure that the lower platen of the MRS slides under the model during horizontal loading. The vertical reaction beams constrain the horizontal displacement of the roof and floor blocks of the seal model. Hence, the applied load is transferred to the horizontal reaction beam and reaction diagonal plates.

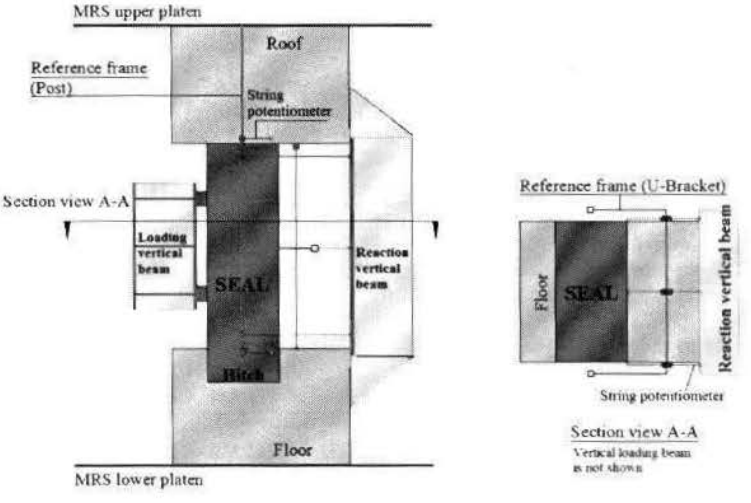

Figure 2 — Schematic drawings for the displacement measurement system.

Seal construction and data collection

Seal model construction begins by casting the roof and floor blocks. Following the concrete cure period, the simulated roof and floor blocks are assembled with a steel frame, and the seal formwork is built between the floor and roof blocks. The seal is cast while the frame is horizontal. The concrete settling was eliminated by: 1) pouring the concrete slowly, 2) tamping the concrete while pouring and 3) tapping the sides of the frame with a hammer. When the seal is cured, the seal model is raised upright using a specially designed rotation frame and a 0.18-t (20-st) crane. The seal test models are constructed square and parallel to within 6 mm (0.25 in.).

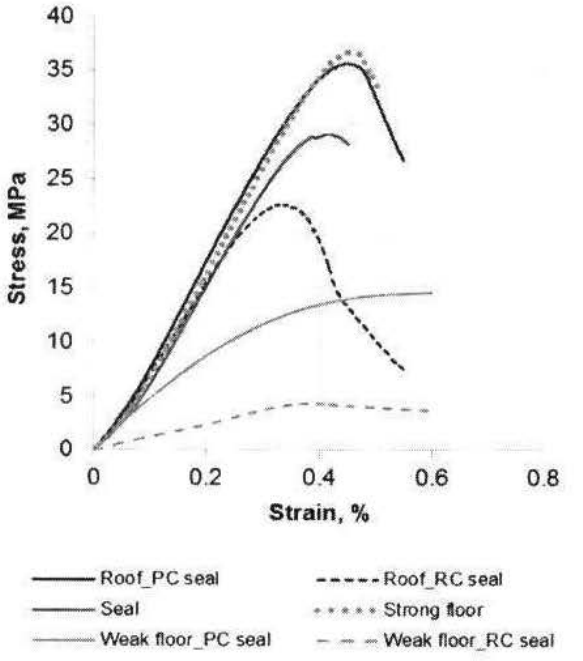

Figure 3 — Stress-strain response of seal, roof and floor specimens for PC and RC seal models.

The instrumentation system for the seal tests (Fig. 2) measures the following:

- Horizontal displacement of the vertical reaction beams.
- Horizontal displacement at the mid-height of the seal.
- Seal slippage at the roof and floor interfaces.
- Roof-to-floor displacement of the test seal.
- Strain at critical members of the MRS seal testing fixture.

The horizontal displacements of the seal model and the vertical reaction beams are measured using linear position transducers (string potentiometers or string pots). A total of 18 string pots are mounted on a reference frame, which is attached to the upper MRS platen and remained stationary during the test (Fig. 2). The reference frame is composed of two 3.3-m- (10.8-ft-) long posts and a horizontal U-bracket connected to the vertical posts at the mid-height of the seal. Six string pots are mounted on each vertical post: three string pots are located at the seal/roof interface to measure seal top, roof block and the top of the reaction beam displacements, as well as three more at the seal/floor interface to measure seal bottom, floor block and the bottom of the reaction beam displacements. Six string pots are mounted on the horizontal bracket: two at each end (left and right) and two at the center of the bracket to measure the displacements at the middle of the seal and the reaction beams. These displacement measurements provided a complete picture of the seal motions during the test including horizontal displacements at the top, bottom and mid-point of the seal along its left and right sides and at its centerline. They also measured displacements along the roof block-seal interface and the floor block-seal interface on the left and right sides.

The shear stiffness of the seal/roof and seal/floor interfaces is determined from the slope of the shear stress versus the seal slippage displacement at the roof and floor interfaces. The rigid body displacements of the roof and floor blocks are subtracted from the measured displacements to obtain the true relative motions of the seal. The resistance function of the seal is obtained by plotting the applied horizontal pressure on the loading face of the seal against the reduced displacement at the middle section of the opposite face of the applied load.

Two string pots are mounted in the roof block and connected to the floor block to monitor the displacement between roof and floor blocks. The roof-to-floor displacement is used to identify the development of arching action in the tested seal.

Two strain gauges are spot welded on each diagonal to further assess loading conditions applied on the seal. Two sets of strain gauges are spot welded on the loading and reaction horizontal beams. These gauges are mounted to ensure that (1) the seal testing fixture remains in the elastic range of the steel at all times during the seal tests and (2) the loads are applied symmetrically and without bending on the seal. Up to the moment of seal failure, the measured strain in the loading horizontal beam (part 2, Fig. 1) was always nearly the same as that in the reaction horizontal beam (part 10, Fig. 1) to within 5%. Similarly, the measured strain in the loading (part 12, Fig. 1) and reaction (part 1, Fig. 1) diagonals, left and right, agreed to within 5%.

Seal testing

Eight experiments were conducted for each plain concrete (PC) and reinforced concrete (RC) seal, considering the full combination of three boundary conditions: hitching, roof-to-floor convergence and floor strength. The nomenclature used in this study for hitching, nonhitching, with-convergence, without-convergence, strong floor and weak floor are H, NH, C, NC, S and W, respectively. As an example, a hitched seal built on strong floor without roof-to-floor convergence is abbreviated as H_NC_S.

The concrete materials used in this study were obtained from a commercial concrete supplier. While casting the roof, seal and floor blocks, samples were poured in cylindrical molds (100 mm by 200 mm) (4 in. by 8 in.). These specimens were cured in the same conditions as the seal model for at least 28 days. The uniaxial compressive strength tests were carried out according to the ASTM D2938-95 (ASTM, 1998). The axial displacement of the sample was measured by the testing machine stroke. Figure 3 shows the stress-strain response of concrete specimens of the seal model components. The mechanical properties of the seal model are summarized in Table 1. Weak floor conditions in a coal mine were simulated using 14.6-MPa (2,111-psi) and 4.36-MPa (632-psi) concrete for PC and RC seals, respectively. Strong floor conditions were simulated using a 36.7-MPa (5,330-psi) concrete. The coal mine roof was simulated using 35.6-MPa (5,170-psi) and 22.7-MPa (3,290-psi) concrete for PC and RC seals, respectively. The PC and RC seals were built using 29.1-MPa (4,220-psi) concrete.

It was not planned to use different roof and floor strengths for PC and RC seals. The simulated strong and weak floors were designed for strengths of 34.5 MPa (5,000 psi) and 6.9 MPa (1,000 psi), respectively, and the roof foundation for a strength of 20.7 MPa (3,000 psi). The PC seal models were made first. Unfortunately, the strength of the delivered concrete of PC foundations was much higher than the requested strengths. To correct this problem for the RC seal models, concrete mix designs were customized for the roof and weak floor foundations of the RC seal models to achieve the desired strengths. The objective of the PC and RC seal tests conducted in this study is to measure the resistance functions of the PC and RC seals and not to compare them.

Table 2 — Measured and calculated seal failure data.

Seal model	PC seals					RC seals				
	Initial cracking					Diagonal failure				
	Vertical pressure, MPa (psi)	Displacement, mm (in.)		Pressure, MPa (psi)		Vertical pressure, MPa (psi)	Displacement, mm (in.)		Pressure, MPa (psi)	
		Test	Model	Test	Model		Test	Model	Test	Model
NH_NC_S	0.18 (25)	0.59 (0.023)	0.56 (0.022)	0.35 (50)	0.32 (47)	0.09 (13)	2.07 (0.082)	3.02 (0.119)	0.30 (43)	0.49 (71)
NH_C_S	0.38 (55)	N.A.	0.55 (0.022)	N.A.	0.41 (59)	1.41 (204)	2.76 (0.109)	3.87 (0.152)	0.52 (75)	0.70 (101)
H_NC_S	0.22 (32)	0.67 (0.026)	0.42 (0.017)	0.37 (54)	0.34 (50)	0.08 (12)	4.22 (0.166)	4.51 (0.178)	0.57 (83)	0.66 (96)
H_C_S	0.78 (112)	0.69 (0.027)	0.49 (0.019)	0.51 (74)	0.53 (76)	1.05 (152)	4.51 (0.177)	5.38 0.212	0.72 (104)	0.83 (121)
NH_NC_W	0.32 (46)	0.39 (0.015)	0.63 (0.025)	0.28 (40)	0.35 (51)	0.04 (6)	14.37 (0.566)	12.96 (0.510)	0.68 (99)	0.69 (99)
NH_C_W	0.87 (126)	0.83 (0.033)	0.50 (0.020)	0.40 (58)	0.51 (74)	1.61 (233)	8.20 (0.323)	8.44 (0.332)	0.77 (111)	0.65 (94)
H_NC_W	0.29 (41)	0.49 (0.019)	0.49 (0.019)	0.29 (41)	0.34 (49)	0.04 (6)	8.83 (0.348)	5.97 (0.235)	0.70 (101)	0.60 (87)
H_C_W	0.84 (121)	0.81 (0.032)	0.47 (0.018)	0.55 (79)	0.49 (71)	0.72 (104)	9.53 (0.375)	6.40 (0.252)	0.75 (109)	0.66 (96)

N.A. not available

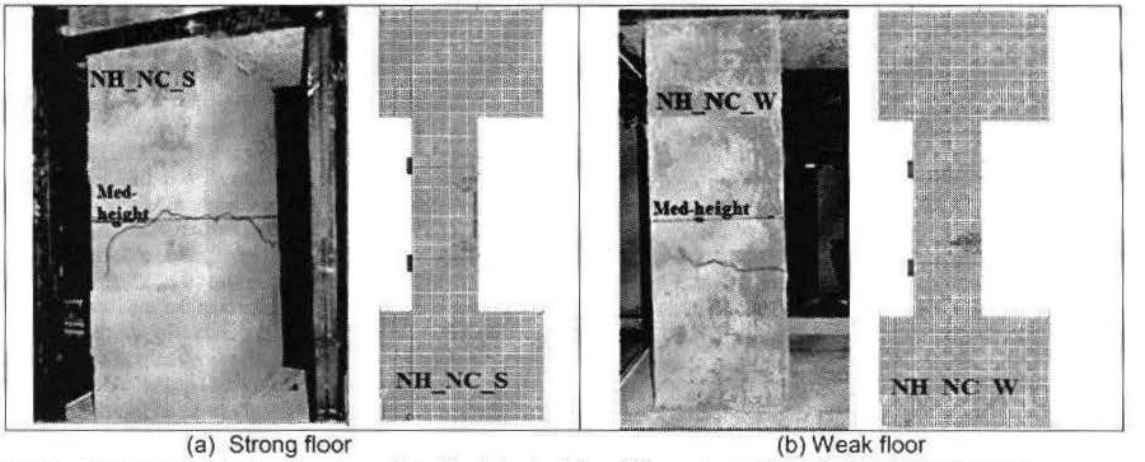

(a) Strong floor (b) Weak floor

Figure 4 — Observed (dark lines) and predicted (red dashed lines) flexural cracking of plain concrete seals.

Plain concrete (PC) seal tests. The PC seal dimension is 1.83-m (6-ft) high by 1.22-m (4-ft) wide by 0.61-m (2-ft) thick. The thickness-to-height ratio of the PC seals is 1/3, which classifies the test seals as deep beams. Therefore, the failure of the seal is mainly rupture at the midspan of the opposite face of loading associated with shear slippage at the interfaces. Roof-to-floor convergence was imposed on the seal model by applying initial vertical loads on the seal model. A summary of applied vertical pressures on the PC seal models is in Table 2.

No sign of failure such as cracking was observed in the roof or floor foundations during any of the PC tests. Except for the NH_C_S test, all other tests have the following characteristics:

- Nonviolent tensile failure was initiated at the mid-span opposite the loaded face of the seal. Figure 4 shows a sample of the rupture patterns of the PC seals for the NH_NC_S and the NH_NC_W tests.
- The rupture was propagated as a single fracture plane toward the loaded face of the seal.
- Ultimate shear strength of the seal/roof and seal/floor interfaces was not achieved. The seal/roof and seal/floor interfaces were intact after the seal testing.
- The initial vertical load applied on the top of the seal model was maintained constant until the rupture initiated, and then arching action was developed in the specimen. The tests were stopped to avoid damage to the horizontal loading and reaction beams in the testing fixture.

The NH_C_S test showed diagonal tension through the seal

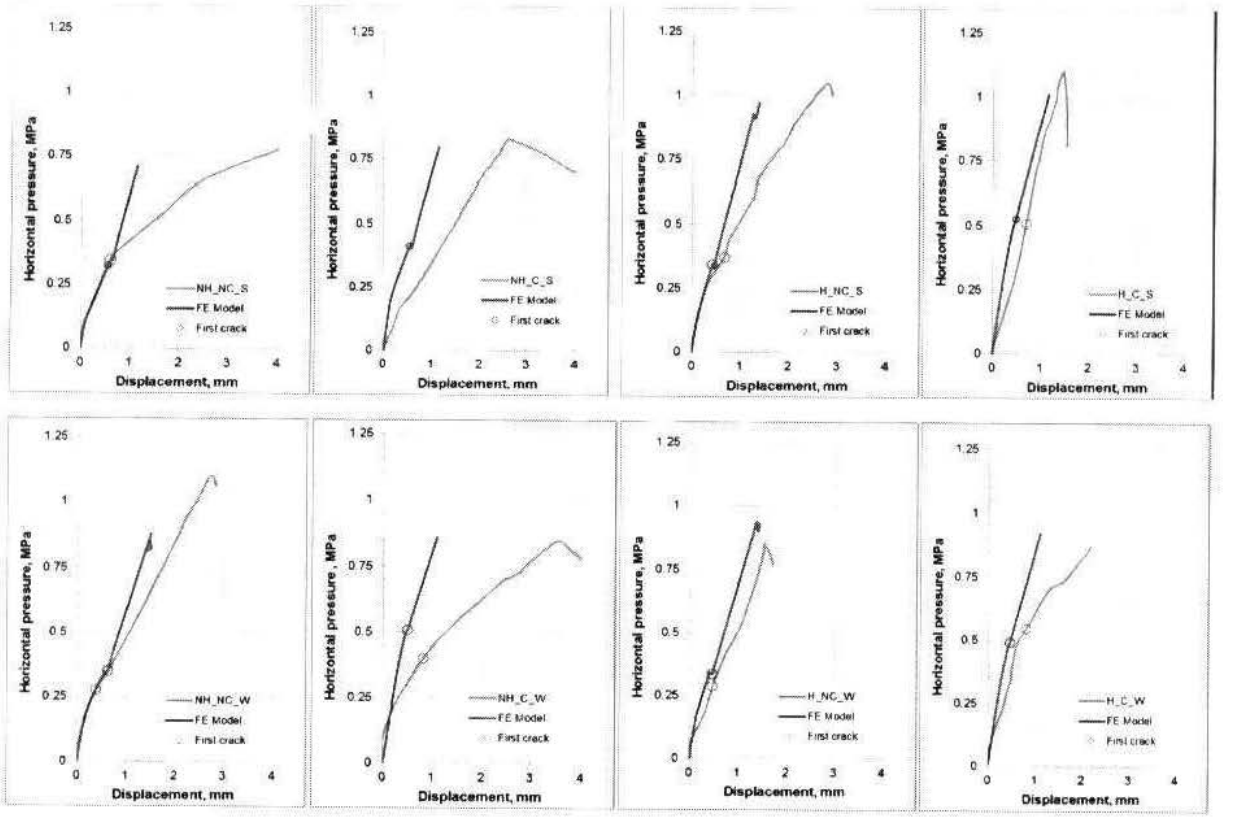

Figure 5 — Measured (blue) and predicted (red) resistance functions of plain concrete seals.

near the floor foundation associated with violent failure. Unlike all of the PC tests, the largest displacement for NH_C_S test was observed at its bottom and significant roof-to-floor displacement was observed during the seal testing. The odd behavior of the NH_C_S test is attributed to the preparation method of this seal model. It was later determined that the roof and floor foundations were out of plane.

Figure 5 shows the measured resistance functions from the PC seal tests. The initiation of tensile cracks opposite the loading face of the seal is denoted by the blue circles. All of the PC tests, except the NH_C_S test, have linear resistance functions up to the initiation of tensile cracking. The measured horizontal displacements at the mid-height of the seal and the applied horizontal pressures at the initiation of tensile cracks are summarized in Table 2. A horizontal seal displacement of 0.39 mm to 0.84 mm (0.015 in. to 0.033 in.) at the mid-height of the seal was enough to initiate a tensile crack at the mid-span of the seal, depending on testing conditions of the seal.

Reinforced concrete (RC) seal tests. The RC seal dimension was 1.83-m (6-ft) high by 1.22-m (4-ft) wide by 0.3-m (1-ft) thick. The RC seals contained two planes of steel reinforcement located 64 mm (2.5 in.) from the faces of the seal. Each reinforcement plane contains four vertical steel bars 16-mm (0.625-in.) diameter spaced at 356 mm (14 in.) and five horizontal steel bars 10-mm (0.375-in.) diameter spaced at 0.3 m (1 ft) for nonhitched seals. Six horizontal steel reinforcements of 10-mm (0.375-in.) diameter were used, spaced at 0.33 m (1 ft) for hitched seals. Vertical dowels of 16-mm (0.625-in.) diameter bars were used to anchor the nonhitched seals into the roof and floor blocks. The vertical and horizontal steel reinforcements have a yield strength of 413 MPa (60,000 psi). The hitched seals are only anchored to the roof foundation. A concrete cover is required to protect steel reinforcement from corrosion. ACI318 (American Concrete Institute) recommends a minimum of 38 mm (1.5 in.) of cover for most structures. Roof-to-floor convergence was imposed on the seal model by applying initial vertical loads on the seal model. A summary of applied vertical pressures on the RC seal models is in Table 2.

Reddy et al. (2011) experimentally observed that, at a low shear span-to-seal thickness ratio (up to two), the shear failure of a reinforced concrete beam without web reinforcement is violent. The shear span of the beam is defined as the beam portion between loading point and support, which is 0.457 m (18 in.) for the tested RC seals. The shear span-to-seal thickness ratio of the tested RC seals is 1.5. Hence, all of the RC seals failed with sudden violent shear failure. Figure 6 shows samples of the shear failure patterns for the NH_NC_S and NH_NC_W tests. The shear cracks initiated at approximately 45° opposite the loading face of the seal and propagated across the neutral axis of the seal before horizontal flexural cracks appeared at the midspan of the seal (Fig. 6). Because of the similar strength of the roof and strong floor foundations, the RC seals built on strong foundations behave as fixed-end beams. Therefore, both top and bottom shear cracks were observed in the RC seals with the strong floor foundations (Fig. 6). For

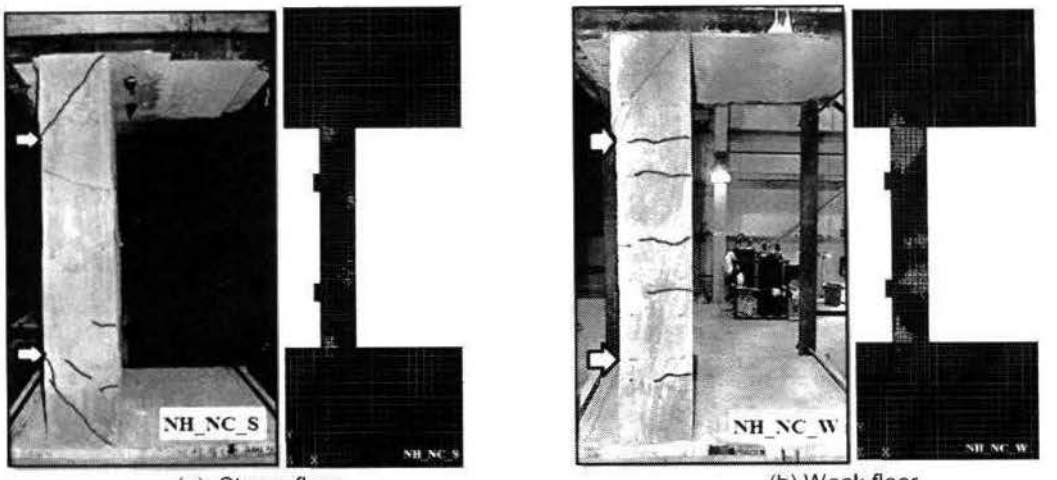

(a) Strong floor (b) Weak floor

Figure 6 — Observed (dark lines) and predicted (green hatched area) diagonal tension cracks for reinforced concrete seals.

RC seals constructed on weak floor foundation, floor heave was observed in the floor opposite the loading face of the RC seal. The RC seals built on weak floor foundations behaved as beams fixed at their top end and partially fixed at their bottom end. Therefore, the majority of the RC seals built on weak floor foundations showed only top shear cracks, but the mid-span flexural cracking was more evident, likely due to higher bending moments at their fixed end. Yielding of the dowel bars was not confirmed in all RC seal tests, but for some tests, such as H_NC_S, yielding of dowel bars was observed.

Figure 7 shows the measured resistance functions from the RC seal tests. The initiation of observed shear failure is denoted by blue circles. The resistance functions of the RC seals built on strong floor foundations are linear up to a horizontal pressure of about 0.21 MPa (30 psi) to 0.28 MPa (40 psi). They became nonlinear until the shear failure is initiated (Fig. 7). Horizontal loading continued until shear failure was achieved and was followed by sudden violent failure of the RC seal (descendent part of the curves). The measured horizontal displacements at the mid-height of the seal and the applied horizontal pressures at the initiation of shear failure are summarized in Table 2. A horizontal seal displacement at the mid-height of the seal between 2.07 mm (0.08 in.) and 4.51 mm (0.17 in.) was enough to initiate shear cracks in the shear span of the RC seals built on a strong floor foundation. The RC seals built on weak floor foundations showed softer resistance functions than those built on strong floor foundations. A horizontal seal displacement at the mid-height of the seal between 8.2 mm (0.32 in.) and 14.37 mm (0.57 in.) was enough to initiate shear cracks in the shear span of the RC seals built on weak floor foundations.

Finite element models for PC and RC seals

ANSYS Ver. 13.0 (2011) was used to simulate the four-point static loading for all the PC and RC seals. The state of stress in the PC seals is plane stress; therefore, a 25-mm- (1-in.-) thick model was used to simulate the PC seals (Fig. 8a). For the RC seals and loading, only one-half of the RC seal is modeled (Fig. 8b) due to the symmetry in cross section. ANSYS Solid65 elements, to be explained later, were used to model the roof, seal and floor of the PC and RC seal tests. Structural beam elements were used to model the dowels and the vertical and horizontal steel bars of RC seals. A perfect bond between the concrete and steel reinforcement was assumed in the RC seal FE models.

The interactions of the roof and floor foundations with the upper and lower platens of the MRS and with the reaction mechanism of the testing frame are modeled as roller supports (Fig. 8). The displacement control approach was used to load the PC and RC seals in the FE models to mimic the displacement controlled seal tests and to avoid the early divergence of the FE models, especially when the concrete begins to crack. The loading mechanism of the testing frame was modeled by applying horizontal displacement at a remote loading point (Fig. 8) located at a distance of 0.65 m (2.13 ft) from the loading plates, which is equal to the distance between the loading plates (part 7, Fig. 1) of the vertical loading beams (part 6, Fig. 1) and the round bar (part 14, Fig. 1). The remote loading point is allowed to move in the x direction and to rotate about the y axis, while all other degrees of freedom are constrained. The loading plates are coupled with the remote loading point. Frictionless contact is defined at the loading plates/seal interfaces. Eight-node brick elements were used to model the loading plates. Elastic steel properties were assigned to the loading plates. The seal models are solved in two steps: (1) a vertical displacement in the z direction equivalent to the initial vertical load is applied on the bottom of the floor block; (2) a horizontal displacement in the x direction is applied on the remote loading point in a manner similar to that in the test program.

Constitutive model of concrete. The constitutive model of the Solid65 element representing the concrete is based on the William-Warnke failure surface (Hauksdóttir, 2007). The element is capable of cracking in three orthogonal directions and crushing. The ability of a crack to transfer the shear stress across its plane is defined by the shear transfer coefficients (β_t and β_c). These coefficients range from 0.0 to 1, with 0.0 representing a smooth crack (no aggregate interlock) and 1 representing a rough crack (full aggregate interlock). Shear transfer coefficients for open and closed cracks were assumed to be 0.3 and 1, respectively (Kachlakev et al., 2001; Vasudevan and Kothandaraman, 2011; Wolanski, 2004). In compression, the Solid65 element could undergo plastic deformation using

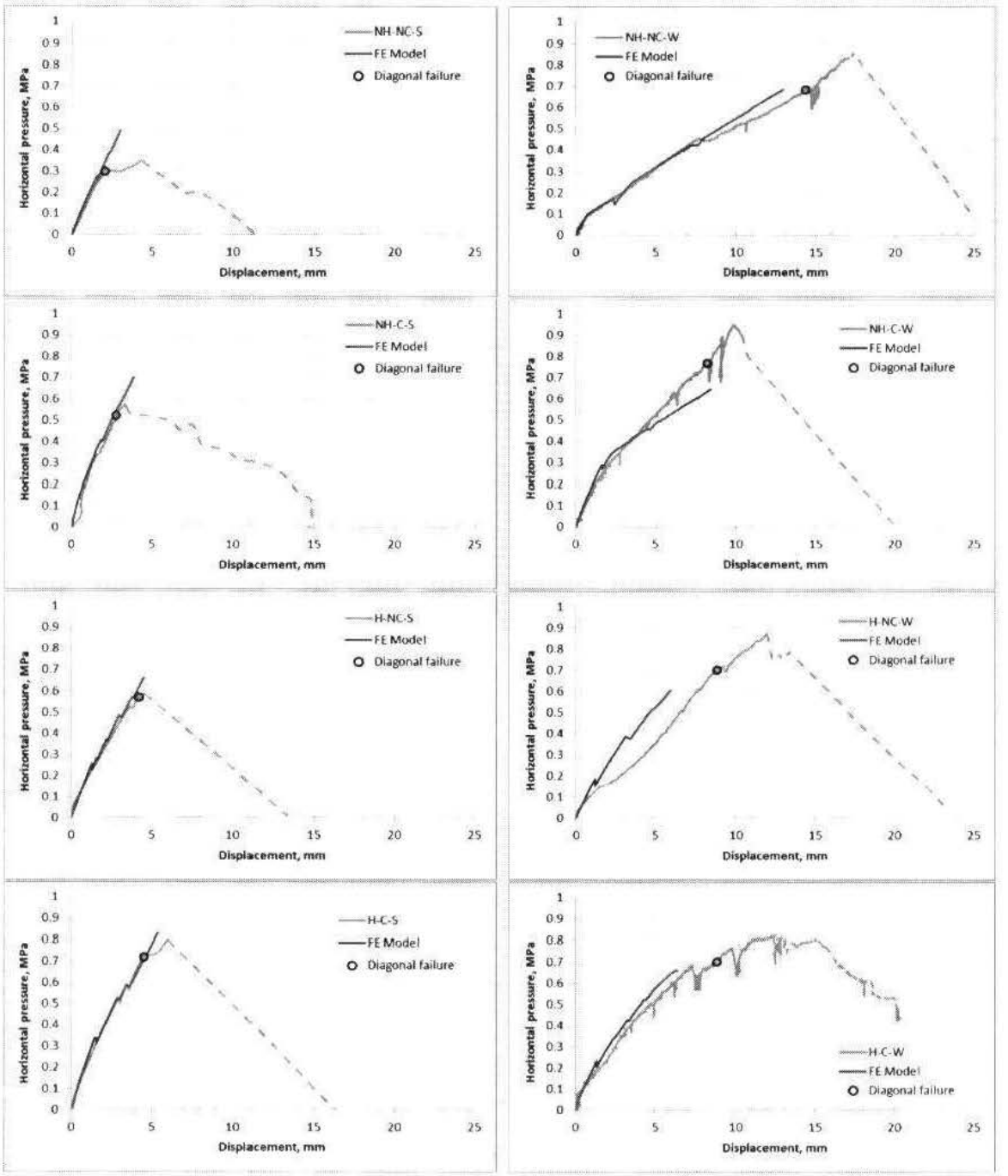

Figure 7 — Measured (blue) and predicted (red) resistance functions of reinforced concrete seals.

Von-Mises failure criterion (ANSYS, 2011) coupled with isotropic work-hardening stress-strain models (Fig. 3).

The direct tensile strength (f_t) of concrete is markedly lower than the compressive strength (f_c). The direct tensile strength of concrete is difficult to measure and can be taken as a fraction of the modulus of rupture (f_r) (Ghaffar, 2005):

$$f_t = 0.3 * f_r \quad (1)$$

The modulus of concrete rupture varies widely but is normally taken in psi as (Chen, 2007):

$$f_r = 7.5 * \sqrt{f_c} \quad (2)$$

The concrete properties used in the finite element models are summarized in Table 1. Young's modulus for the roof, seal and floor of the test specimen were experimentally determined. The Poisson's ratio of all components of the seal model was assumed to be 0.3 (Vasudevan and Kothandaraman, 2011; Wolanski, 2004).

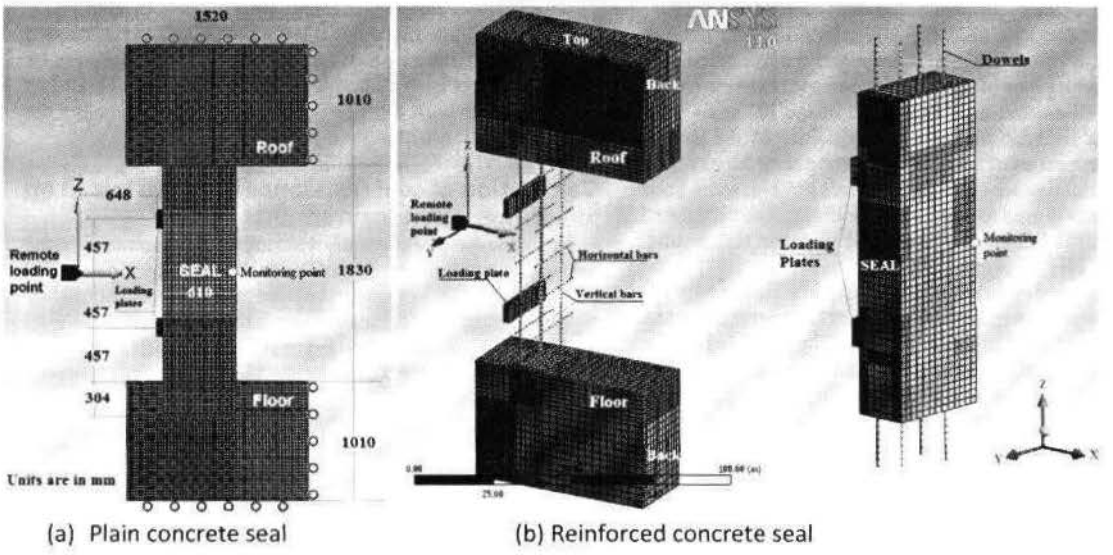

Figure 8 — FE model of plain and reinforced concrete seals.

The tensile rupture was the dominant mode of failure for PC seal tests; therefore, the direct tensile strength was assigned to seal material of PC models. On the other hand, the shear failure was the dominant mode of failure for RC seal tests. Hence, the tensile strength of seal material is not considered to be a critical input for RC seal models. Therefore, the modulus of rupture was assigned to seal material of RC seal models to avoid modeling divergence. Similarly, the tensile strengths of the roof and floor foundations were estimated from the modulus of rupture. The concrete crushing capability of Solid65 elements was suppressed to avoid modeling divergence (Kachlakev et al., 2001; Vasudevan and Kothandaraman, 2011; Wolanski, 2004; Saifullah et al., 2011; Al-Azzawi et al., 2010). The ANSYS defaults of Solid65 elements were assumed for the rest of the concrete material constants. The Von-Mises plasticity model was used to simulate the steel bars in RC seals. A Poisson's ratio of 0.3 is assumed for the steel reinforcement and the modulus of elasticity is 212 GPa (30 x 10^6 psi) (Barth and Woo, 2006).

Modeling of the seal/foundation interface. The horizontal loading of nonhitched plain concrete seals (NH_NC_S, NH_C_S, NH_NC_W, NH_C_W) is very similar to that used in large-scale double shear tests (Mogi, 2007). Therefore, these tests were used to estimate the shear stiffness of the seal/roof and seal/floor interfaces. The average shear stiffness of the seal/roof interface is estimated to be 0.96 MPa/mm (3,550 psi/in.). The average shear stiffness of seal/strong floor and seal/weak floor interfaces are estimated to be 1.29 MPa/mm (4,730 psi/in.) and 0.87 MPa/mm (3,200 psi/in.), respectively. The cohesions of the seal/roof and seal/strong-floor interfaces were determined by laboratory direct shear tests as 3.22 MPa (467 psi) and 1.95 MPa (283 psi), respectively. The compressive strength of roof block is less than that of strong floor block, but the cohesion of the seal/roof interface is greater than the seal/strong floor interface. Similar results were experimentally found by Shin and Wan (2010), where the bond strength of the cold joint between new and old concrete blocks was measured. The friction coefficient of the seal/roof and seal/floor interface and the cohesion of seal/weak floor interface of RC seals are assumed to ensure the best match between the measured and estimated seal resistance functions. The ACI building code (318.83) gives the range of the coefficient of friction along the interface between new and existing concrete as 0.6 to 1.1 (ACI). A summary of the properties of the seal/roof and seal/floor interfaces used in the finite element models is shown in Table 1. The mechanical properties of the seal/roof interface (Table 1) characterize the perfect bond between roof and seal, which is applicable for the seal models built in this study.

Comparison of FE models with experimental results

The FE models of PC and RC seals are calibrated by being compared with their corresponding seal tests. The comparison is based on the following measures:

- Failure pattern of the seal,
- Failure horizontal pressure and horizontal displacement at the mid-height of the seal – defined by the rupture crack initiation for PC seals and the shear failure for RC seals, and
- Resistance function of the seal.

Figure 4 shows the calculated initial rupture cracks of PC seals for NH_NC_S and NH_NC_W models. The calculated

initial tensile cracks are plotted as red dashes. The figure shows that the concrete cracking started at the outer fiber of the mid-section of the seal, then propagated perpendicularly toward the loading face of the seal. Symmetric concrete cracking is observed around the mid-height of the PC seals built on strong floor foundations, which is explained by the similar mechanical properties of the roof and strong floor blocks. The calculated initial rupture cracks of PC seals built on weak floor foundations was biased toward the floor block. The calculated failure pattern of PC seals agrees well with the test results, except for the NH_C_S test.

The resistance functions of the PC seals estimated by FE models compared with their corresponding resistance functions determined from the seal tests are shown in Fig. 5. The red circles represent the onset of concrete cracking in the FE model. The estimated horizontal pressure and the mid-height seal displacement at crack initiation from the FE models agree well with the test results. Except for the NH_C_S and NH_C_W seals, the estimated and measured resistance functions are almost identical. The NH_C_S test underestimated the stiffness and strength of the tested seal because the roof and floor blocks of the seal model were out of plane. The FE model overestimated the stiffness of the NH_C_W seal after the onset of rupture. This behavior is attributed to the continuity assumption of the concrete material model where the smeared crack analogy for tension cracking was used in the Solid65 elements. For most of the PC seal tests, the calculated and the measured horizontal pressure at crack initiation are very close (Table 2).

Figure 6 shows the calculated failure patterns of the RC seals for NH_NC_S and NH_NC_W models. The cracks in the RC seal models are plotted as green dashes. Concrete cracking started at the mid-section of the RC seal opposite the loading face. The cracks were more pronounced for the RC seals built on weak floor foundations. Diagonal tension cracks are calculated through the seal thickness at its shear spans. Both top and bottom diagonal tension cracks are observed in the RC seals built on strong floor foundations. For RC seals built on a weak floor foundation, the diagonal tension cracks are only well-pronounced at the top of the seal. As shown in Fig. 6, the calculated failure patterns from the FE models for RC seals agree well with observations from the seal tests.

The resistance functions of the RC seals estimated by the FE models are compared with their corresponding resistance functions determined from the seal tests in Fig. 7. Except for the NH_C_W and H_NC_W seals, the estimated and measured resistance functions are almost identical. A total failure of the RC seal is identified where the solution fails to converge even with a very small displacement increment (Kachlakev et al., 2001; Wolanski, 2004). The FE models overestimated the shear strength of the RC seals built on strong foundation. This behavior is attributed to the continuity assumption of concrete material, where the smeared crack analogy for tension cracking was used in the RC seal FE models. As a result of the continuity assumption of concrete material, an arch action was developed in the FE models of RC seals, especially for the strong floor foundation. For practical seal design, the seal strength gained because of the arch action should be ignored because the rigid boundaries that are required to develop the arch action in the seal are not existent. The geology (bedding planes, cracks, soft material, etc.) of mine roof and floor will prevent the development of the arch action in mine seals. On the other hand, because of numerical instability of the RC seal models built on weak floor foundations, the FE models underestimate the shear strength of seal models built on weak floor foundations by about 15% (Table 2). Weak floor foundations were not able to provide suitable support for the RC seal because of floor yielding. Significant displacements were measured and calculated for the RC seal built on weak foundations, which caused more seal cracking (Fig. 6). Therefore, certain measures should be taken for mine seals built on weak floors—e.g., replacing the weak foundation with a strong plain concrete.

Calculation of seal resistance function based on experimental measurements

From these experimentally determined measurements of the load-deformation behavior of model seals and the calibrated FE model of the seal behavior, the resistance functions for proposed plug and RC seals were determined. A 1.8-m (6-ft) high entry was assumed to demonstrate the application of the calibrated finite element model for these approximate seals.

Plug seal. For a 1.83-m- (6-ft-) high entry, a plug seal of 2.74-m- (9-ft-) thick plain concrete and a compressive strength of 20.7 MPa (3,000 psi) were examined. A strong floor foundation for a nonhitched plug seal is assumed and no roof-to-floor convergence is applied. The modulus of elasticity (E_c) of the seal in psi is estimated as follows (Chen, 2007):

$$E_c = 57{,}000\sqrt{f_c} \tag{3}$$

The stress-strain relationship of the plug seal material is estimated by Eq. (4). The mechanical properties of the roof and floor and the seal/roof and seal/floor interfaces used in the finite element model of the plug seal model are presented in Table 1. In practice, it is difficult to have a perfect bond between the plug seal and the roof stratum. Therefore, the cohesion of the seal/roof interface was assumed to be zero and the shear resistance at the seal/roof interface is only governed by the friction component in the FE model.

The nonlinear stress-strain relationship for the weak floor foundation of the plug seal was defined as follows (Kachlakev et al., 2001):

$$\sigma = \frac{E_c * \varepsilon}{1 + \left(\frac{\varepsilon}{\varepsilon_0}\right)^2} \tag{4}$$

$$E_c = \frac{2f_c}{\varepsilon_0} \tag{5}$$

where

σ = stress as a function of strain, ε.
f_c = ultimate compressive strength, psi.
ε_0 = strain at the ultimate compressive strength.
E_c = Young's modulus.

Figure 9a shows the calculated resistance function for the 1.83-m- (6-ft-) high by 2.74-m- (9-ft-) thick plug seal. No cracking was predicted in the plug seal. At an early stage of loading, 0.1 MPa (14.5 psi), the seal/roof slippage occurred. At a horizontal pressure of 2.46 MPa (357 psi) and a horizontal displacement of 2.07 mm (0.08 in.), slippage at the seal/floor interface occurred without stop. The plug seal stiffness is calculated as 1.19 MPa/mm (4,440 psi/in.). Based on the PC seal experiments and the calibrated FE models, a bilinear resistance function was calculated for a plug seal with a compressive strength of 20.7 MPa (3,000 psi) and a width-to-height ratio of 1.5. The calculated resistance function can be used in a SDOF code such as SBEDS to calculate the dynamic response of the assumed seal subjected to any of the design pressure-time curves

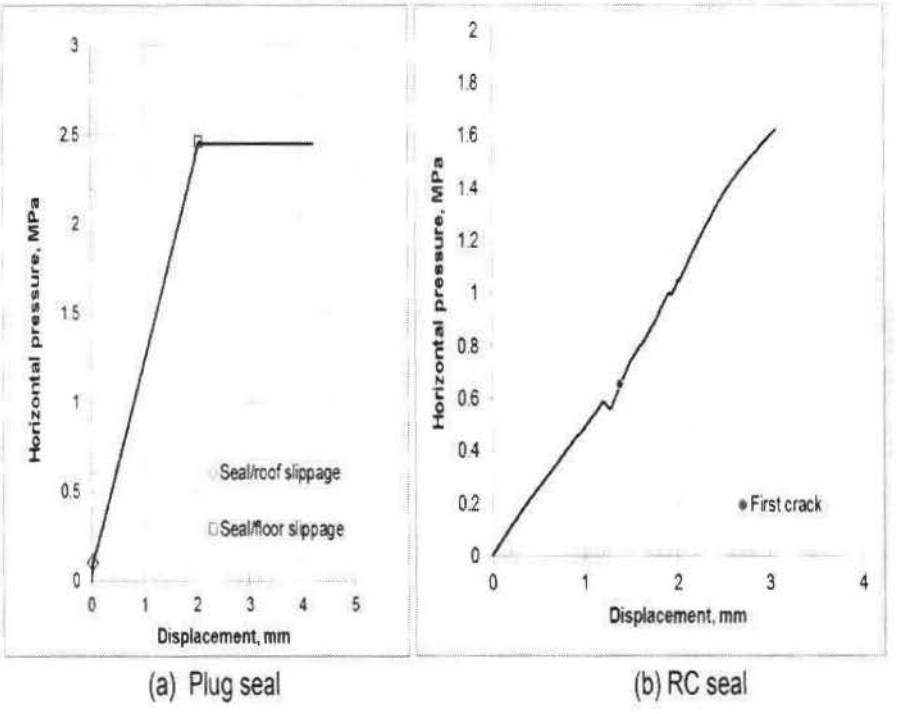

Figure 9 — Estimated resistance functions for plug and RC seals.

listed in 30 CFR 75.335 (*Federal Register*, 2008).

Reinforced concrete seal. For a 1.83-m- (6-ft-) high entry, a reinforced concrete seal of 0.56-m- (1.83-ft-) thick and a compressive strength of 31.0 MPa (4,500 psi) were assumed. A strong floor for a nonhitched RC seal is assumed and no roof-to-floor convergence was applied. Steel bars of 25-mm (1-in.) diameter were used for dowels and vertical reinforcement and steel bars of 16-mm (0.625-in.) diameter were used for horizontal reinforcement. No shear reinforcement members were used. The layout of dowels and vertical and horizontal reinforcements is the same as for the RC seals used in this study (Fig. 8b). The modulus of elasticity (E_c) of the concrete in psi was estimated using Eq. (3). The stress-strain relationship of the RC seal material was estimated by Eq. (4) and (5). The tensile strength of the RC seal was estimated by Eq. (4). A summary of the properties of the roof and floor and the seal/roof and seal/floor interfaces used in the finite element model of the RC seal model is shown in Table 1.

Figure 9b shows the estimated resistance function for the reinforced concrete seal design. The initiation of cracking developed at a horizontal pressure of 0.65 MPa (94 psi) and at horizontal displacement of 1.39 mm (0.05 in.). The average RC seal stiffness is calculated as 0.53 MPa/mm (1,940 psi/in.). Based on the RC seal experiments and the calibrated FE models, a nonlinear resistance function of the assumed RC seal was calculated. The calculated resistance function of the RC seal can be used in any SDOF code such as SBEDS to calculate the dynamic response of the assumed seal subjected to any of the design pressure-time curves listed in 30 CFR 75.335 (*Federal Register*, 2008).

Summary

The objective of this study was to develop engineering data for use in the design of plain and reinforced concrete mine seals. The test data is used to calibrate FE models that, in turn, are used to determine the resistance functions for these test seals and for the ultimate use in single degree of freedom analysis tools such as SBEDS.

Based on this ASTM E72-02 method, NIOSH researchers designed a testing fixture using a four-point load, which was applied until failure to 1.22-m- (4-ft-) wide by 1.83-m- (6-ft-) high seals. A lateral design load of 40 MN (900,000 lbf) was selected for design of the fixture to apply a static pressure of 1.66 MPa (240 psi) on the seal.

Sixteen large-scale tests of PC and RC seals were conducted. The tests considered the effects of floor strength, hitching condition and roof-to-floor convergence on the resistance functions of the seals. The resistance functions and failure patterns were recorded for all the tests.

Weak floor conditions in a coal mine were simulated using 14.6 MPa (2,100 psi) and 4.36 MPa (632 psi) concrete for PC and RC seals, respectively. Strong floor conditions were simulated using a 36.7-MPa (5,330-psi) concrete. The coal mine roof was simulated using 35.6-MPa (5,170-psi) and 22.7-MPa (3,290-psi) concrete for PC and RC seals, respectively. The PC and RC seals were built using 29.1-MPa (4,220-psi) concrete. The cohesions of the seal/roof, seal/strong floor and seal/weak floor interfaces were 3.22 MPa (467 psi), 1.95 MPa (283 psi) and 0.34 MPa (50 psi), respectively. The mechanical properties

of the seal/roof interface characterize a perfect bond between roof and seal, which is representative for the seal models built in this study. The average shear stiffness of the seal/roof interface is calculated from the large-scale seal tests as 0.96 MPa/mm (3,550 psi/in.). The average shear stiffness of strong and weak floor interfaces was found to be 1.29 MPa/mm (4,730 psi/in.) and 0.87 MPa/mm (3,200 psi/in.), respectively.

Calibrated FE models for PC and RC seals were developed using ANSYS Ver. 13. The input data for the FE seal models, such as Young's modulus, compressive strength, stress-strain relationships, etc., were obtained from laboratory-scale material testing, and the shear stiffness of the seal/roof and seal/floor interfaces were obtained from the large-scale seal tests. With very limited engineering-based assumptions and a single set of data, both the PC and the RC FE seal models successfully calculated the measured resistance functions and failure patterns for a wide range of boundary conditions.

Based on the PC seal experiments and the calibrated FE models, a bilinear resistance function of a plug seal with a compressive strength of 20.7 MPa (3,000 psi) and width-to-height ratio of 1.5 was calculated. Also, a nonlinear resistance function of an RC seal was calculated. The calibrated FE models can be used to calculate the resistance functions for a wide range of plug and RC seal designs. The calculated resistance functions of these seals can be used in any SDOF code such as SBEDS to calculate the dynamic response of the assumed seals subjected to any of the design pressure-time curves listed in 30 CFR 75.335 (*Federal Register*, 2008).

Currently, similar experimental and modeling studies are being conducted to determine and validate the resistance functions of pumpable cement foam seals and concrete masonry unit seals glued together with polyurethane.

Acknowledgments

The authors acknowledge the invaluable NIOSH OMSHR personnel whose contributions made the seal testing program possible: James Addis, Frank Karnack and Donald Sellers, physical science technicians, for assembly of the seal testing fixture, casting the foundations, building the PC and RC seals, moving the seal model in/out of the MRS and assembly of the displacement measuring devices on the seal. The authors acknowledge the following mechanical technicians with Wolverine (a NIOSH contractor) for manufacturing the seal testing fixture and making the seal model frame and the foundation forms: Bernard Lambie, Brandin Lambie and Timothy Glad (lead).

Disclaimer

The findings and conclusions in this report are those of the authors and do not necessarily represent the views of the National Institute for Occupational Safety and Health.

References

Al-Azzawi, A.A., Mahdy, A.H., and Farhan, O. Sh., 2010, "Finite element analysis of deep beams on nonlinear elastic foundations," *Journal of the Serbian Society for Computational Mechanics*, Vol. 4, No. 2, pp. 13-42.

American Concrete Institute, *Building Code Requirements for Reinforced Concrete*, ACI 318, Farmington Hills, MI.

American Society of Civil Engineers, 1997, *Design of Blast Resistance Building in Petrochemical Facilities*, ASCE, New York, pp. 6-23.

American Society for Testing and Materials, 1998, "Concrete and aggregates," ASTM, Volume 04.02.

ASTM Designation E 72-02, 2002, "Standard test methods of conducting strength tests of panels for building construction," *Annual Book of ASTM Standards*.

ANSYS Ver. 13, 2011, *Finite Element Analysis System*, ANSYS, Inc., Canonsburg, Pennsylvania.

Army, U.S., 1990, "Structures to Resist the Effects of Accentual Explosions," Headquarters Department, TM 5-1300.

Army Corps of Engineers, U.S., "Single-degree-of-freedom Blast Effects Design Spreadsheet (SBEDS)," Protective Design Center, https://pdc.usace.army.mil/software/sbeds, accessed June 2013.

Barth, K.E. and Wu, H., 2006, "Efficient nonlinear finite element modeling of slab on steel stringer bridges," *Finite Elements in Analysis and Design*, Vol. 42, No. 14, pp. 1304-1313.

Chen, W.F., 2007, *Plasticity in Reinforced Concrete*, John Wiley & Sons, Inc., New York, NY.

Federal Register, 2008, "Rules and Regulations Sealing of Abandoned Areas-Final Rule," Title 30 CFR Part 75.335 CFR, *Code of Federal Regulations*, Washington DC: U.S. Government Printing Office, Office of the Federal Register 73(76), Friday, April 18, 2008.

Gadde, M.M., Beerbower, D.A. and Rusnak, J.A., 2008, "A simplified approach to coal mine sealdesign," *12th U.S. North American Mine Ventilation Symposium*.

Ghaffar, A., Chaudhry, M.A. and Kamran, M.A., 2005, "A new approach for measurement of tensile strength of concrete," *Journal of Research (Science)*, Bahauddin Zakariya University, Multan, Pakistan, Vol. 16, No. 1, pp. 1-9.

Hauksdóttir, B., 2007, Analysis of a Reinforced Concrete Shear Wall, M. Sc. Thesis, Technical University of Denmark.

Kachlakev, D.I., Miller, T., Yim, S., Chansawat, K., Potisuk, T., 2001, "Finite element modeling of reinforced concrete structures strengthened with FRP laminates," California Polytechnic State University, San Luis Obispo, CA and Oregon State University, Corvallis, OR for Oregon Department of Transportation, May.

Kallu, R.R., Mohamed, K. Morsy, Zingano, A., and Turner, D., 2007, "Effect of roof convergence on stability of underground mine seal subjected to explosion loading - numerical approach," *26th International Conference on Ground Control in Mining*, Morgantown, West Virginia, 370 pp.

Mine Safety and Health Administration, 2012, Approved Seals under the Final Rule, http://www.msha.gov/Seals/SealsSingleSource2007.asp, accessed August 2012.

Mogi, K., 2007, *Experimental Rock Mechanics*, Taylor & Francis Group, London, UK.

Mohamed, K. Morsy, Yassien, A., and Peng, S., 2009, "Cementitious plug seal/rock interface under static and dynamic loadings," *Proceedings of the 80th Shock & Vibration Symposium*, San Diego, CA.

Mutton, I.V. and Remennikov, A., 2010, "Designing explosion rated ventilation seals for coal mines using high-fidelity physics-based computer modeling," *Underground Coal Operators' Conference*, University of Wollongong Research online.

Reddy, S.L., Rao, R.N.V., and Rao, G.T.D., 2011, "Evaluation of shear resistance of high strength concrete beams without web reinforcement using ANSYS," *ARPN Journal of Engineering and Applied Sciences*, February, Vol. 6, No. 2.

Saifullah, I., Hossain, M.A., Uddin, S.M.K., Khan, M.R.A., and Amin, M.A., 2011 "Nonlinear analysis of RC beam for different shear reinforcement patterns by finite element analysis," *International Journal of Civil & Environmental Engineering*, IJCEE-IJENS, Vol. 11, No. 01, pp. 86-97.

Shin, H. and Wan, Z., 2010, "Interfacial properties between new and old concretes," *2nd International Conference on Sustainable Construction Materials and Technology*, Ancona, Italy.

Vasudevan, G. and Kothandaraman, S., 2011, "Parametric study on nonlinear finite element analysis on flexural behavior of RC beams using ANSYS," *International Journal of Civil and Structural Engineering*, Vol. 2, No. 1.

Westman, E., 2007, "Comparison of arched and flat seal designs using finite element analysis," SME Annual Meeting, February 25-28, Denver, CO, Preprint 07-106.

Wolanski, A.J., 2004, Flexural Behavior of Reinforced and Pre Stressed Concrete Beams Using Finite Element Analysis, M. Sc. Thesis, Marquette University.

Zipf, R.K., Weiss, E.S., Harteis, S.P. and Sapko, M.J., 2009, Compendium of Structural Testing Data for 20-psi Coal Mine Seals, IC 9515, U.S. Department of Health and Human Services, National Institute for Occupational Safety and Health.

Zipf, R.K. and Mohamed, K. Morsy, 2009, "Design and analysis of a new method to test mine seals," *Proceedings of the 80th Shock & Vibration Symposium*, San Diego, CA.